LANDTECHNIK 75(4), 2020, 176–193

DOI:10.15150/lt.2020.3244

LANDTECHNIK
AGRICULTURAL ENGINEERING

Model for the analysis of the influence of the dynamic load shift on the traction behavior of a pipe laying machine

David Wildner, Thomas Herlitzius, Torsten Berg

The trenchless laying of collector pipes in the field of near-surface geothermal systems (agrothermics) requires the development of a functional demonstrator of a mobile laying unit. In this paper, the basics for the analysis of the controllability of a future traction management system of such machines are considered. It is shown how the interactions within the considered machine system and the interdependency between machine and soil can be approximately described using suitable models. The modeling is based on multi-body simulations for the kinematics and the chassis as well as on semi-empirical approaches for the tensile force-slip behavior of the crawler track. For describing the tool-soil interaction a mathematical-physical approach for subsoilers is used in addition. As a summary, an overall model for analyzing the influence of machine and tool parameters on traction behavior is shown. This approach can be used for the development and the analysis of a traction management system based on the active control of tool parameters.

Keywords
Traction, Simulation, Crawler Track, Traction Management System

In the field of renewable energies, the innovative procedure called "agrothermics" describes the usage of near-surface geothermal energy, preferably below arable areas. Collector pipes are laid in a large area and at a depth of two meters in order to use the thermal energy. The average annual temperature at these depths is approximately 10 degrees. The maximum differences are up to ± 6 K (Grosa et al. 2018). Subsequently, the collector pipes are connected to pumping stations via larger storage pipes. This system forms a closed circuit. For the transfer of the thermal energy a water-glycol mixture is used. After connecting consumers and producers of thermal energy to this system, it is defined as a cold-heat network. The addition “cold” enables differentiation from conventional heat supply, in which the heat loss from power plants is usually used. The particular collector systems can be connected separately and can work as heat source, heat sink or as an accumulator. The thermal energy in this system could be used by other consumers such as private households. Heat pumps could increase the heat level for use within the heating/cooling system or water heating. Another advantage could be the possible double usage of arable areas. Plant cultivation should not be affected. This enables the energy commercialization by the owner or the tenant of the land. In former projects, two pilot plants were built in Neumarkt (Upper Palatinate, Germany) and in Wüstenrot (Baden-Württemberg, Germany) (Grosa et al. 2018, König 2017). In these projects, first experiences with the laying of collector pipes as well as knowledge about the practical usage of the agrothermics could be gained. This technology was prototyped in the system of thermal and energy supply along with the project “EnVisaGe” in the munici-

received 16 April 2020 | accepted 11 September 2020| published 7 October 2020

pality of "Wüstenrot" for the first time. The feasibility and functional reliability of the system could be demonstrated for a couple years of operation by now (König 2017).

Based on the experience and the results of former projects, the large-scale trenchless laying of the collector pipes using ploughing technology was identified as the economical and technical optimal solution. Known trench cutting processes have no relevance in agricultural used fields, because of the undesirable vertical exchange of soil. According to Grosa et al. (2018), construction machines enable working depths of up to two meters. The further development in the context of agrothermics focused on the development of specialized laying tools. After the first field tests with these tools, the limits of available base machines were shown (Grosa et al. 2018):

- Lack of controllability of the pulling force
- Unavailable/insufficient pipe logistics
- Insufficient possibilities to react of soil disturbances
- Inadequate documentation possibilities

Based on this discrepancy of the state of development between the laying tools and the base machines, current research is focusing the development of a functional demonstrator of such a pipe laying machine system. In this context, the functionality and the controllability of the transferable pulling force of the machine are considered in this paper. The focus is specifically on the dynamic load shift of the vertical load from the tool on the crawler track. This effect was mentioned by Kuhlewind (1932) and Janert (1955), but was never quantified. Kalbheim (2005) described a resulting increase in the transferable tensile force, considering trench cutters and trenchless working ploughs. Thus, the following investigations show the development of a model for analyzing the interrelationships using the functional demonstrator as an example. The system is divided into the subsystems of kinematics, chassis and the description of the interdependencies between the crawler track and the soil as well as the tool and the soil. Using these models and specific simplifications, the influence of various parameters on the traction behavior of the machine is analyzed. A traction management system based on the results could be developed in perspective. In this context, defined tool parameters are adjusted to enable control of the traction behavior of the crawler track. A better understanding of these relationships also offers the possibility of reducing the operating weight and the dimensions of the machine accordingly.

Analysis of the machine system

The concept of the machine considered as an example is shown in Figure 1. The base machine consists of the upper and lower section (2) with engine compartment, operator's place and track undercarriage. The coupling of the special laying tools (6) is realized through a newly developed kinematics (4), which was specially designed for this application. It was developed to optimize the insertion and lifting process of the tool. The line of the resulting tool force (3) describes the dynamic load transfer from the laying tool to the crawler track. In the context of pipe logistics, the laying machine carries its own pipe reel (1). The pipes are fed to the laying tool via the pipe driver unit (5). Inside the tool, they are guided to a depth of two meters below ground and leave the tool at the lower rear end.

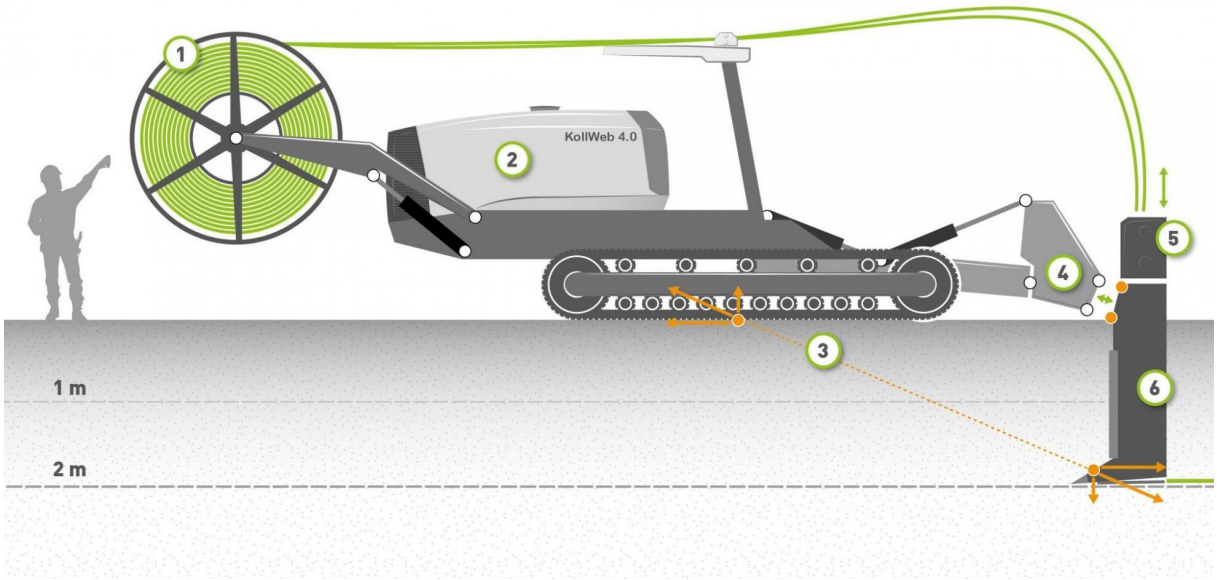

Figure 1: Machine concept

For the modeling of the machine, the system is reduced to the kinematics and the chassis as essential subsystems. In addition, the system boundaries are expanded to take into account the interactions between the soil and the crawler track as well as the soil and the laying tool.

During the laying process, the tool is pulled into the soil by the machine moving forward. Inside the tool, the pipes are guided to a depth of two meters below ground and leave the tool at the lower rear end. The laying tool is characterized by a working depth that is much larger than the width. Compared to the narrow shank, the foot of the tool is relatively wide. This is necessary for leading multiple pipes. In addition, these wide feet increase the vertical pull-in force (Herlitzius et al. 2015). With the exception of special cases, the hydraulic cylinders of the kinematics are hydraulically locked with check valves during the laying process. The resulting tool forces are transferred to the base machine through the kinematics. The loads are distributed to the ground by two crawler tracks (Figure 2). The connection is made via a pendulum bridge and a pivot pin for transverse compensation of the movements between the left and right chassis. For the transfer of the vertical loads into the soil, they are distributed on 12 rollers as well as the drive wheel and the idler wheel. The resulting horizontal forces must be applied by the two hydraulic drives. In addition, a planetary gear is connected to each of the hydraulic motors. The connection between the track undercarriage and the soil is represented through a crawler track with 57 base plates per side. The demonstrator is equipped with alternately arranged 1- and 3-web base plates.

Figure 2 : Lateral view of the track undercarriage – (© TU Dresden, Chair of Agricultural Systems and Technology)

Modeling

In the context of system modeling, Figure 3 must first be considered. This visualization shows all relationships, projected on one plane. Neglecting the lateral loads, the resulting tool forces are represented by the vertical and horizontal process forces. At first, the point of force application must be considered. The determination of the position is based on analysis of the displacement areas of the tool in the horizontal and vertical direction. The position in the vertical direction is determined by calculating the center of gravity of the tool surface that is projected onto the vertical plane. This procedure applies analogously to the horizontal direction and the horizontal plane. In the current state of research this assumption leads to sufficient accuracy. Measured values from the machine could be used to calculate the influence of a varying position on the load distribution on the track undercarriage. The kinematics are coupled to the base machine via two connection points. The connection of the track undercarriage to the frame is to be regarded as rigid in the first approximation. The interface between the rollers of the undercarriage and the crawler track is represented by the roller loads.

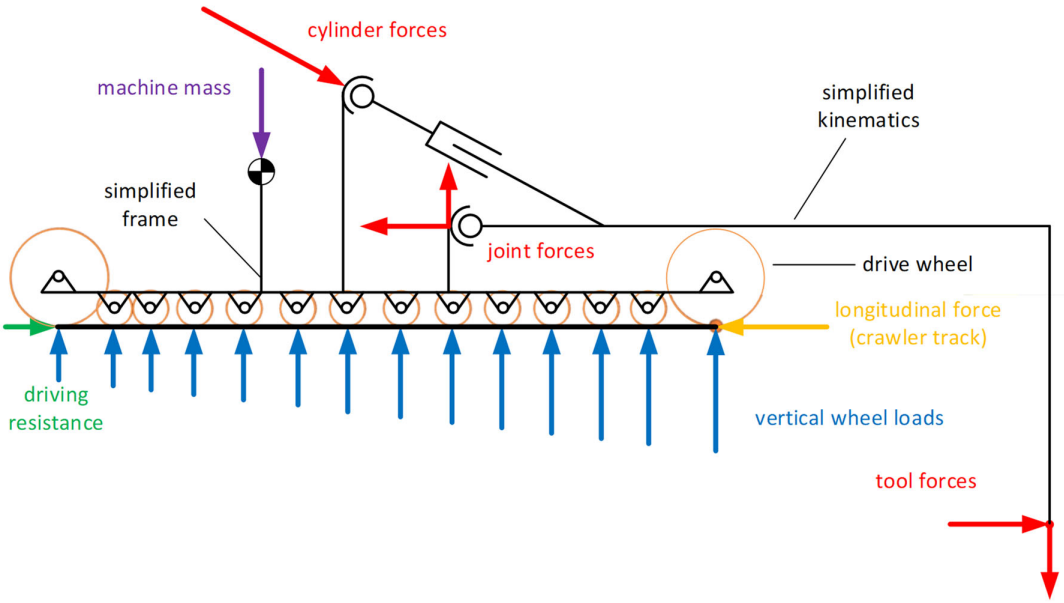

Figure 3: Overview of the system model

Modeling – tool-soil interaction

On the other hand, realistic quantification of the amount of horizontal and vertical tool force is more difficult. Throughout the historical development, the trenchless laying of pipes, which resulted from the mole and mole pipe drainage, placed very high demands on the required performance of the tractors. These pulling machines have always been the limiting factor. Voss and Zimmermann (1974) first investigated the tensile forces required for trenchless-working tools. In this context, the authors analyzed different tools for a working depth of up to 1.3 m. As a result, the authors were able to show the linear increase in the required pulling force to a depth of 1.3 m. In summary, this work only allowed a comparison of the tensile force required for different tool types. Tracing back to specific tool parameters was not the subject of the work.

By contrast, a large number of publications were already available at this time regarding the recording of horizontal and vertical forces on the plough body. As a difference the conventional plough is working relatively near to the soil surface. In addition, the main task is to loosen and turn the soil. Measurements on plough bodies were carried out up to a maximum depth of 35 cm (Getzlaff 1951). This mixes the soil thoroughly and heaps it up on surface of the soil. However, the mechanisms during trenchless laying at significantly greater working depths are different – more compaction, less displacement. The results of such investigations are therefore not easily transferable. In contrast to ploughs, a trenchless-working tool is characterized by the fact that the working depth is significantly greater in relation to the tool width. As a consequence, as the working depth increases, less soil is heaped up on the surface. Furthermore, the soil that is displaced by the foot is getting more compressed.

To derive theoretical descriptions of the forces of drainage tools, Demian (1974) examined simple angle and flat chisels. Measurements were carried out up to a maximum depth of 35 cm. The author then developed an approach for how the results obtained can be extrapolated by applying the similarity mechanics to real-size tools and a working depth of up to 200 cm. This approach neglects the increasing compaction of the soil and the smaller amount of soil that raises up on the ground.

Godwin and Spoor (1977) described the balance of forces on a narrow, inclined plate. The usage of this theory requires the determination of the non-dimensional N-factors, which depend on the angle of friction between steel and soil ρ, the angle of the internal friction φ and the cohesion c. The author‘s theory is based on observations that the fracture behavior of the soil changes from a defined depth. Above this critical value (“crescent failure”), the soil is displaced forward, upwards and in the lateral direction. However, if the working depth is greater (“lateral failure”), there are no longer any soil movements in the vertical direction. As a result, the authors developed a theory for the approximate calculation of the critical depth as well as the vertical and horizontal forces. The calculation results were validated to a working depth of 230 mm. Many other mathematical descriptions of tillage resistances are based on this approach according to Godwin and Spoor. However, it is not possible to apply these theories to tools with a significantly greater working depth for the reasons mentioned above. Further investigations in the context of deep loosening technology therefore focused on more specific approaches.

In this context, Balaton (1990) developed a mathematical-physical approach for subsoilers that have much greater working depths. This theory is also based on Godwin and Spoor's critical depth. The following prerequisites initially apply within this theory:

- Working depth significantly larger than width of the tool
- Tool compresses soil at working depth and the soil cracks and loosens at maximum stress
- Crack surface is approximated as a cone

Balaton first differentiates between the resistance forces on the foot and the shank of the tool. Furthermore, according to the expected behavior, it is assumed that the soil is raised to the height h by the cutting angle at the coulter tip. During this process, the soil is compressed. This is counteracted by the weight of the soil, the cohesive forces, the inertia of the soil material, the resistance at the cut edge of the coulter and the reaction force within the soil. According to the author‘s investigations, the inertia was not significant and was neglected. Furthermore, the fracture angle shows only a minimal dependence on the cohesion of the soil. Subsequently, he defines this angle with $\psi = 45°$.

The horizontal resistance at the tool foot R_x is calculated taking into account the geometry, the density of the soil γ, the angle of the internal friction φ, the cohesion c and the friction angle between the steel and the soil ρ (equation 1):

$$R_x = \frac{\gamma * g * \left\{(b + H * \cot(\psi)) * \left[\frac{H^2}{2} * \cot(\psi) + \left(H - \frac{h}{2}\right) * h * \cot(\beta)\right]\right\}}{\cot(\beta + \rho) + \cot(\psi + \varphi)} + \frac{c * H * \{b * [1 + \cot(\psi) * \cot(\psi + \varphi)] + H * [tan^2(\psi) + \cot(\psi) * \cot(\psi + \varphi)]\}}{\cot(\beta + \rho) + \cot(\psi + \varphi)} \quad \text{(Eq. 1)}$$

R_x: horizontal resistance at the tool foot
γ: density of the soil
φ: angle of the internal friction
c: cohesion
ρ: friction angle between the steel and the soil
ψ: fracture angle
H: working depth

The same applies to the vertical part of the resistance at the foot R_z (equation 2):

$$R_z = \frac{\gamma * g * \left\{(b + H * \cot(\psi)) * \left[\frac{H^2}{2} * \cot(\psi) + \left(H - \frac{h}{2}\right) * h * \cot(\beta)\right]\right\}}{1 + \tan(\beta + \rho) + \cot(\psi + \varphi)} + \frac{c * H * \{b * [1 + \cot(\psi) * \cot(\psi + \varphi)] + H * [tan^2(\psi) + \cot(\psi) * \cot(\psi + \varphi)]\}}{1 + \tan(\beta + \rho) + \cot(\psi + \varphi)} \quad \text{(Eq. 2)}$$

R_z: vertical resistance at the tool foot
b: width of the tool foot

The detailed derivations can be found in Balaton (1990). Balaton determines the resistance component of the shank R_{ks} as the sum of the cutting force on the cutting edge and the frictional force, which acts on the sides due to the ground pressure. The author initially only looks at shank shapes in a straight and not in a curved version. He attributes this to the excessive number of dependencies known from the literature. Only the inclination of the straight shaft would have to be taken into account with the corresponding angle. The individual parts of the tool shank are calculated according to Balaton, taking into account specific forces (equation 3). In this context, k_1 is defined as specific resistance due to soil deformation. The factor k_2 corresponds to the specific ground pressure on the side surfaces. The biggest problem here is the known dependency of such factors on the geometry of the tool as well as on the soil parameters.

$$R_{ks} = (H - h) * \left\{k_1 * b_{ks} * \left[1 + tan(\rho) * \cot\left(\frac{\alpha}{2}\right)\right] + 2 * k_2 * s * \tan(\rho)\right\} \quad \text{(Eq. 3)}$$

R_{ks}: resistance component of the shank
b_{ks}: width of the shank
s: length of the shank

Assuming defined tool and soil parameters, a first analytical description of these dependencies for trenchless working tools according to Balaton is possible. This approach is sufficient for the desired investigations. It is initially not necessary to calculate the most precise possible force curves for defined soils. The focus is rather on a tendency description of the tool behavior and the effects on the traction behavior when changing different parameters (e.g. width of the tool foot or angle of inclination). The influence of the working speed on the tool forces can initially be neglected under the assumed very low real travel speed of the machine system of 0.2 to 0.8 m s^{-1}.

Modeling – kinematics

The kinematics are modeled using a nonlinear multi-body system (Figure 4). In perspective, this also enables the analysis of various installation depths. Within the environment of SimulationX® (ESI ITI GmbH), the modeling was based on the CAD data of real components. The respective elements are mapped with the corresponding inertias and their masses reduced to the center of gravity. The cylinders were integrated on the basis of configurable elements from the multi-body library from SimulationX®. Analogous to the CAD geometries, the masses and inertias of these linear actuators including fluid masses are also taken into account. Manufacturer values for the pressure-dependent static and sliding friction have been implemented for modeling the mechanical efficiency of the hydraulic cylinders. Damping forces proportional to speed are also taken into account.

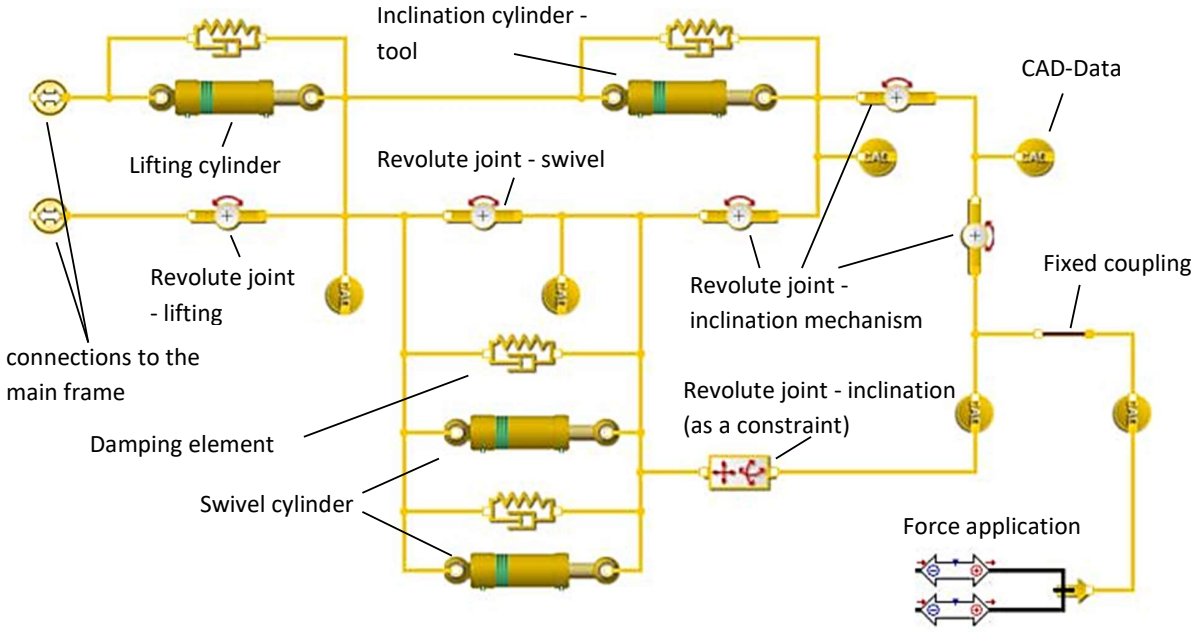

Figure 4: Model of the kinematics without the visualization of the hydraulic connections

Modeling – chassis/ load distribution

During the development of a mechanical model, the 14 bearing forces of the individual rollers result in a system that is underdetermined. This task was therefore calculated using a nonlinear 2D mechanical model in the environment of SimulationX®. The individual rollers were modeled according to the geometric conditions as contact elements (circle-straight line) (Figure 5). These elements enable minimal movement during the elastic contact process. A downward directed load accordingly leads to a reaction force. The distance covered during this elastic contact process is calculated from the model of an ideal spring and is therefore proportional to the force. In the developed model, the associated stiffness was assumed to be 100 kN mm^{-1}. Excessive rigidity would result in this system approaching the above mentioned problem with 14 fixed bearings and would not be able to be solved. A stiffness value that is too low would lead to unrealistic movements. The individual rollers can move smoothly on the straight line and also lift off from it under the action of a defined vertical force.

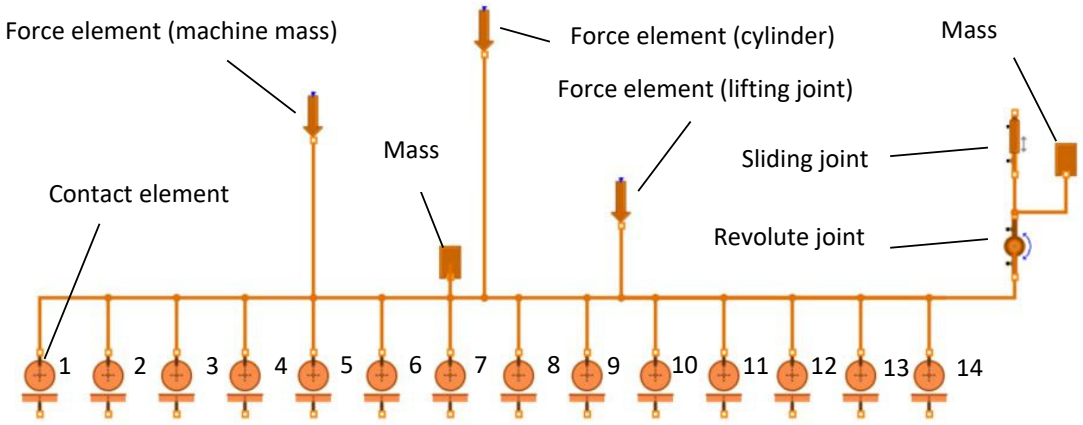

Figure 5: model of the chassis (load distribution)

In order to enable the required movements for the calculation, the corresponding degrees of freedom must be implemented in the model. From Figure 1 and Figure 3, the contact point under the drive wheel is identified as the tilting edge. This is the point around which the vehicle “rears up” under additional strain from the tool. This is modeled using a serial arrangement of a revolute and a sliding joint. The latter enables the entire vehicle to perform a translatory movement in the vertical direction. This is necessary because the point of rotation is directly located under the driving wheel (roller 14) and otherwise the vertical movement of this roller would always be constant and thus independent of the load. The revolute joint enables the rotation around the movable contact point.

The force application via the interfaces to the kinematics and the center of gravity is realized via 2D force elements. By neglecting the tool-soil model and with a simplified assumption of constant horizontal $F_{L,h}$ and vertical $F_{L,v}$ tool forces, exemplary load distributions can be determined for different cases (Figure 6). The forces shown correspond to the sum of the left and right track undercarriage. This linear function of the roller loads is the basis for the operating point-dependent calculations of the traction behavior of the crawler track.

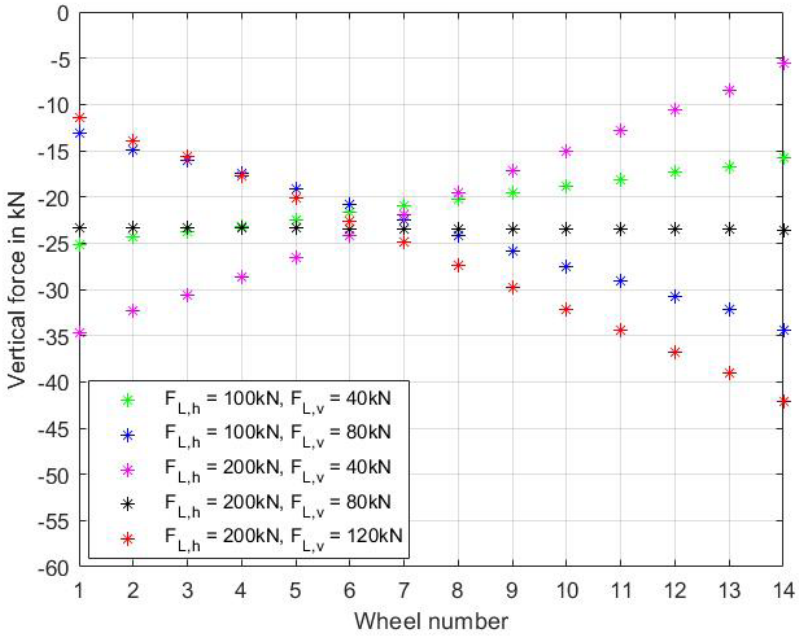

Figure 6: Load distribution

Modeling – traction

With regard to the calculations of the traction-slip behavior, a linear stress distribution under the crawler track is assumed. The stress peaks under the roller elements are neglected. Based on this simplification, the following procedure is used to determine the resulting stress curve $\sigma_N(x)$ along the longitudinal axis of the vehicle. The resulting roller forces (see Figure 2) are first summarized in a vector $\vec{F}_{R,v}$. In the second step it is assumed that the normal stress under the crawler track changes proportionally to the vertical force. For this purpose, the corresponding mean values of roller force $F_{R,v,MW}$ and stress $\sigma_{N,MW}$ must be determined. To calculate the average stress, the total vertical force must be referred on the contact area of both crawler tracks ($A_{CT} = 2 * b_{CT} * l_{CT}$):

$$F_{R,v,MW} = \frac{\sum_1^{14}\left(\vec{F}_{R,v}(i)\right)}{14} \qquad \text{(Eq. 4)}$$

$$\sigma_{N,MW} = \frac{\sum_1^{14}\left(\vec{F}_{R,v}(i)\right)}{2 * b_{CT} * l_{CT}} \qquad \text{(Eq. 5)}$$

$F_{R,v,MW}$: mean values of roller force
$\sigma_{N,MW}$: mean values of stress
b_{CT}: width of the crawler track
l_{CT}: length of the crawler track

In order to determine the linear function of the normal stress, the required parameters must be determined using appropriate ratio equations. The stress value at roll 1 $\sigma_N(1)$, which also corresponds to the offset of the stress equation $\sigma_N(x)$, is thus defined as:

$$\sigma_N(1) = n_\sigma = \sigma_{N,MW} * \frac{\vec{F}_{R,v}(1)}{F_{R,v,MW}} \quad \text{(Eq. 6)}$$

The increase in the function $\sigma_N(x)$ can be determined from the difference in the normal stress under the first and the last roll, referred on the length of the crawler track (equation 7):

$$m_\sigma = \left(\vec{F}_{R,v}(1) - \vec{F}_{R,v}(14)\right) * \frac{\sigma_{N,MW}}{F_{R,v,MW}} * \frac{1}{l_{CT}} \quad \text{(Eq. 7)}$$

The following applies to the function of the normal stress $\sigma_N(x)$ with the running coordinate $0 < x < l_{CT}$ (equation 8):

$$\sigma_N(x) = m_\sigma * x + n_\sigma \quad \text{(Eq. 8)}$$

The description of the relationship between the normal stress distribution and the traction-slip behavior, bases on the fundamental work of Bekker (1956, 1960, 1969) and Wong (2010). These semi-empirical approaches are based on the theory of passive earth pressure according to Terzaghi (1943). The operating point-dependent maximum tensile force $F_{Z,max}$ of the crawler track depends on the chain contact area A_{CT} and on the maximum shear resistance τ_{max} of the soil, which counteracts the horizontal force caused by the webs of the track (equation 9). The maximum shear resistance is to be expressed according to Mohr's stress circle by the cohesion c, the effective normal stress σ_N and the angle of the internal friction of the soil φ.

$$F_{Z,max} = A_{CT} * \tau_{max} = A_{CT} * (c + \sigma_N * \tan(\varphi)) \quad \text{(Eq. 9)}$$

$F_{Z,max}$: maximum tensile force
τ_{max}: *maximum shear resistance*
A_{CT}: chain contact area
c: cohesion
σ_N: normal stress
φ: angle of internal friction

The mentioned relationship can only be used for a stationary vehicle. During the movement of a crawler vehicle, the chain slip would have to be taken into account when determining the maximum transferable tractive force. According to Bekker (1969), it is assumed that all the webs move in one plane and thus shear the soil at the same depth. As a result of the constant drive slip along the crawler track, there is a linear increase in the shear displacement j as a function of the slip, described by the running coordinate x (equation 10). The latter is defined as the distance to the front of the vehicle. In this context, i corresponds to the slip between the crawler track v_{CT} and the real vehicle speed v_v.

$$j = 1 - \frac{v_v}{v_{CT}} * x = i * x \quad \text{(Eq. 10)}$$

j: shear displacement
v_{CT}: crawler track speed
v_v: vehicle speed

The dependency of the shear stress τ on the deformations is described in the theoretical soil mechanics by corresponding relationships between shear stress and shear displacement. When a maximum is exceeded, the strength of dense, non-cohesive and stiff, cohesive soils will drop to a reduced value, the so-called residual shear strength (Engel and Lauer 2017, Lang et al. 2017, Kunze et al. 2009). Tests on substrates that show such behavior with a pronounced stress maximum have carried out by Wong (1983) and Wong and Preston-Thomas (1983). These relationships between shear stress and shear displacement could be demonstrated in the context of snow cover and different types of clay. Based on the first mathematical descriptions of these curves by Bekker (1956) and further developments by Kacigin and Guskov (1968), Oida (1979) developed equation 11:

$$\frac{\tau}{\tau_{Max}} = K_R * \left(1 - \frac{\sqrt{1-K_R} * \left(1 + \frac{\sqrt{1-K_R}-1}{K_R} \right)^{\frac{j}{K_W}}}{\sqrt{1-K_R} * \left(1 - \frac{2}{K_R} \right) + \frac{2}{K_R} - 2} \right) * \left(1 - \left(1 + \frac{\sqrt{1-K_R}-1}{K_R} \right)^{\frac{j}{K_W}} \right) \qquad \text{(Eq. 11)}$$

K_R: ratio of the residual shear strength to the maximum
K_W: shear displacement at the maximum shear stress
j: shear displacement

In this formula, j defines the shear displacement, K_R the ratio of the residual shear strength to the maximum and K_W the shear displacement at the maximum shear stress. With this equation, the shear stress behavior, referred to the maximum value, is to be described mathematically as a function of empirically determined constants. With the exception of the independent variable j, the other parameters are to be determined from corresponding tests. According to Wong (2010), K_W can normally be extracted relatively easily from the measured curves. On the other hand, the determination of the relative residual shear strength is mostly prone to errors due to the non-smooth curves. Wong (2010) developed iterative methods to minimize the error.

Janosi and Hanamoto (1961) also developed equation 12 for soils that do not have a pronounced maximum shear stress over the shear displacement. In the studies on the shear stress behavior of soils, Wong and Preston-Thomas (1983) showed that this behavior applies to different types of sand, saturated clay, fresh snow and peat and that equation 12 approximates the real measured curves very well. The factor K is called the shear deformation parameter and defines the shear displacement at maximum shear stress.

$$\frac{\tau}{\tau_{Max}} = 1 - e^{-\frac{j}{K}} \qquad \text{(Eq. 12)}$$

In addition to the behavior already described, there are also soils which, after the stress maximum has been exceeded and with increasing deformation, show a reduction in the shear stress to $\tau = 0$. This characteristic is typical for fens. According to Wong and Preston-Thomas (1983), this behavior can be represented very well by equation 13. In this formula, K_W describes the shear displacement at maximum shear stress.

$$\frac{\tau}{\tau_{Max}} = \frac{j}{K_W} * e^{1-\frac{j}{K_W}} \quad \text{(Eq. 13)}$$

According to Wong (2010), equation 9 would thus be extended by the soil-dependent relationship between shear stress and shear displacement τ/τ_{Max} in order to determine the maximum tensile force. However, it must be taken into account that the relationships shown by the author assume a constant distribution of normal stress. Accordingly, the derived function of the normal stress distribution must also be considered. It is also taken into account that there are two crawler tracks with the width b_{CT}:

$$F_{Trak,max} = 2 * b_{CT} * \int_0^s (\sigma_N(x) * \tan\varphi + c) * \frac{\tau}{\tau_{Max}}(x) * dx \quad \text{(Eq. 14)}$$

In the context of this paper, defined reference soils are considered based on the relationships shown and according to Equation 14. The description of these soils to be used as examples is based on the investigations made by (Wong 2010). The author analyzed a large number of soils and documented the empirically determined constants. This database enables a first estimation of the tendency of the traction-slip behavior on different soils and with different process and machine parameters.

In addition to the traction-slip behavior, the soil-dependent external driving resistances must also be taken into account within the model. These depend accordingly on the sinkage of the track undercarriage into the ground. The mathematical relationship between the local vertical displacement and the normal stress is to be described by equation 15 according to Wong (2010). The determination of the required soil constants is based on an automated determination procedure (Wong 1980, Wong et al. 1981). Prior work had been done by Bekker (1960) and Reece (1965). High slip would also cause the vehicle to dig into the ground. This so-called slip-sinkage is neglected in the following, because low values for the drive slip are initially to be aimed during the laying operation.

$$\sigma_N = \left(k''_c + b * k''_\varphi\right) * \left(\frac{z}{b}\right)^n \quad \text{(Eq. 15)}$$

In this work, the sinkage z is to be determined accordingly from the resulting normal stress. Furthermore, there is no constant distribution of normal stress. Taking equation 8 into account, equation 16 follows from equation 15:

$$(x) = b_{CT} * \left(\frac{m_\sigma * x + n_\sigma}{k''_c + b_{CT} * k''_\varphi}\right)^{1/n} \quad \text{(Eq. 16)}$$

According to Bekker (1956), soil resistances can also be divided into compaction and bulldozing resistances. The compaction resistance on a track undercarriage results from the necessary compression of the soil during the movement. According to Bekker, this can be determined analogously to the work W_V, which would have to be done so that a vehicle with a given contact area sinks to the depth z_{CT} (equation 17).

$$W_V = b_{CT} * l_{CT} * \int_0^{z_{CT}} \sigma_N(z) * dz \qquad \text{(Eq. 17)}$$

The compression work W_V can also be represented as a product of the length of the contact area l_{CT} and the required force F_V. The force can thus be calculated as follows (equation 18):

$$F_V = \frac{W_V}{l_{CT}} = b_{CT} * \int_0^{z_{CT}} \sigma_N(z) * dz \qquad \text{(Eq. 18)}$$

The described relationship applies accordingly in that case that the stress has to be determined from the sinkage by means of a functional relationship ($\sigma_N = f(z)$). This formula also assumes a constant distribution of normal stress under the crawler track. In this context, the associated sinkage is defined by the depth z_{CT}. In this work, the normal stress results from the load distribution and as a function of the running coordinate x. The relationship between sinkage and stress is described by equation 16. The calculation is therefore carried out in the reverse order. The stress value $\sigma_{N,k}$ at the point $x = k$ is assigned to the sinkage z_k. As a result, the integral of equation 18 would be simplified.

Furthermore, based on the Bekker equivalence analysis, the gutter is divided into many infinitesimally small parts. The work, due to the volumes to be compressed, results from the sum of the individual parts. This procedure is particularly necessary when there is no even distribution of normal stress. In this case, the products $\sigma_{N,i} * z_i$ of the individual infinitesimal areas with the length dx and the width b_{CT} are added and result in the work W_V (equation 19). It is also taken into account that there are two crawler tracks with the width b_{CT}:

$$W_v = 2 * b_{CT} * \sum_{i=1}^{N} \sigma_{N,i} * z_i * dx \qquad \text{(Eq. 19)}$$

According to equation 17 and 19, the following applies to the compression force (equation 20):

$$F_V = \frac{W_V}{l_{CT}} = \frac{2 * b_{CT}}{l_{CT}} * \sum_{i=1}^{N} \sigma_{N,i} * z_i * dx \qquad \text{(Eq. 20)}$$

This relationship applies accordingly to the procedure in this work and in determining the normal stress distribution depending on the load distribution on the chassis. The number of values N results from the total length of the crawler track l_{CT} and the selected step size dx for determining the pairs $\sigma_{N,i}$ and z_i.

Bekker (1960) also identified the so-called bulldozing resistance on very soft ground. This effect is based on a very high sinkage on the front of the vehicle. As a consequence, the chain has to displace the soil before they can be overrun. According to (Wong 2010), the approaches for describing this resistance are based on the theory of passive earth pressure. A derivation of corresponding equations can be omitted, since the mean ground pressure of the machine considered in this work and consequently its sinkage are very low. The bulldozing resistance is therefore neglected.

The forces from air and acceleration resistance known from driving dynamics should be listed as additional parts of the external driving resistance. However, due to the low driving speeds of the

machine type, air resistance does not require consideration. In the context of the quasi-static analysis in this work, the acceleration components can also be neglected. A gradient resistance would have to be taken into account accordingly.

Finally, in the context of modeling the transmission of the tensile force, the simplifications associated with the chosen approach are summarized:

1. All webs of the crawler track move in the same plane
   It is assumed that the webs move at the same depth in the ground and thus shear off the soil at the same height. The aforementioned theories of the authors are based on this assumption and leads to the described linear increase in shear displacement along the longitudinal axis of the crawler track. According to Dörfler (1995), discrepancies between theoretical calculations and field tests, which can be traced back to this state of affairs, are particularly evident in very soft soils and large slip sinkage. Due to the large contact area of the crawler track and the resulting low ground pressure, this assumption can be accepted with sufficient accuracy to calculate the tendential tractive force behavior of the machine system.
2. Chain pitch / distance between the webs correspond to optimal value
   According to the underlying theory, this approach is based on the theory of passive earth pressure. Based on these theoretical backgrounds, it is necessary for the sliding lines to overlap in the passive Rankine sliding zones in order to utilize the optimal shear strength. Consequently, the distance between the webs should be matched to this soil-dependent value (Dörfler 1995, Merhof and Hackbarth 2015, Wong 2010). Assuming a chain with links of only one type (e.g. only 1-track links), the distance between them should have a value according to equation 21. In the considered machine system, a chain consisting of only 1-web elements would come close to this requirement. On the other hand, no concrete statements can be made as to how this situation should be assessed for a chain with 1- and 3-web elements. For the studies carried out in this work on the qualitative change in tensile force in various operating states, this condition is considered to be approximately fulfilled.

$$l_{web} = \frac{h_{web}}{\tan\left(45° - {}^{\varphi}/_{2}\right)} \qquad \text{(Eq. 21)}$$

3. The influence of the frictional forces on the traction cannot be calculated separately
   Within the applied theory it is assumed that the tensile force on the crawler track is generated almost exclusively by the shear stress. The shear strengths in the soil are calculated using the locally resulting normal stresses, which depend on the existing vertical force distribution on the crawler track. A possible influence of the friction forces between the chain and the soil cannot be determined separately. Although the authors achieve good results with this approach, the non-explicit consideration of the friction component contradicts the experience values.
   The application of the model based on concrete measured values, which requires an iterative adjustment of the empirical parameters, must therefore be expanded by an additional friction component. This procedure enables a further degree of freedom to calculate the sufficiently precise traction behavior. Furthermore, the presented model approach would have to be optimized with the implementation of extensive field studies on the influence of the friction component.

4. Speed-independent consideration
   The used theoretical relationships do not take into account the effects of the shear rate on the shear stress curves. In the context of this work, this is initially neglected, since the driving speed of the machine system is very low with a range of 0,2 to 0,8 m s^{-1}
5. Linear distributed normal stress
   In order to determine tendential changes in tensile force, the contact stress under the crawler track in relation to the roller loads was assumed to be linearly distributed. In the context of the qualitative traction considerations, this approach is to be accepted as a good approximation. When analyzing the actual compressive stress distributions or damage compaction in the soil, the actual uneven distribution with the load peaks under the rollers would have to be determined accordingly.

Results

In the previous explanations it was shown how the traction behavior of a pipe laying unit depending on process and machine parameters can be described as a model. The modeling required a separation into the subsystems tool-soil interaction, kinematics, load distribution and traction behavior. The load distribution and the kinematics were mapped using nonlinear multi-body models. On the other hand, the modeling of the interaction between tool and soil as well as crawler track and soil was based on mathematical-physical and semi-empirical approaches that are known from the literature. These descriptions are based on a large number of defined simplifications regarding real behavior. With regard to the planned further use of these models, these simplifications can be accepted. As described at the beginning, these models are used to carry out preliminary studies on the basic static control behavior as well as the limits and the effects of a traction management system. In this context, the most precise possible calculations on defined soils are not necessary. The focus is on studies regarding the qualitative behavior of the controlled system. Based on the results of extensive field tests, the models would have to be optimized and expanded accordingly.

The loads on the tool, respectively the possible soil parameters, are initially not related to the existing soil properties on the crawler track. This is useful due to the assumption that the soil properties at the tool do not always correlate with those at the crawler track. In the worst case, high traction requirements are faced with poor conditions for force transmission at the crawler track (e.g. due to the weather). For this reason, these two parts are considered separately from each other. In perspective, this enables the investigation of different constellations of required tractive effort and traction properties.

In this context, Figure 7 shows exemplary tensile force-slip curves for a defined reference soil. The parameterization of the soil to be driven on was carried out according to equation 11. This corresponds to a soil with a pronounced maximum shear stress and subsequent reduction to the residual shear stress. The machine mass corresponds to m = 25,3 t and the center of gravity is 2839 mm from the drive wheel. With regard to the tool-soil interaction, constant values for the horizontal $F_{L,h}$ and vertical $F_{L,V}$ tool force were initially assumed in a simplified manner. Thus, the diagram shows the maximum horizontal tool force that has to be transmitted through the crawler track with different vertical forces. Based on this, further investigations regarding the concept development of a traction force management system and the identification of a suitable adjustment actuator on the tool would

be possible. This must always be viewed in the context of different reference soils and process requirements.

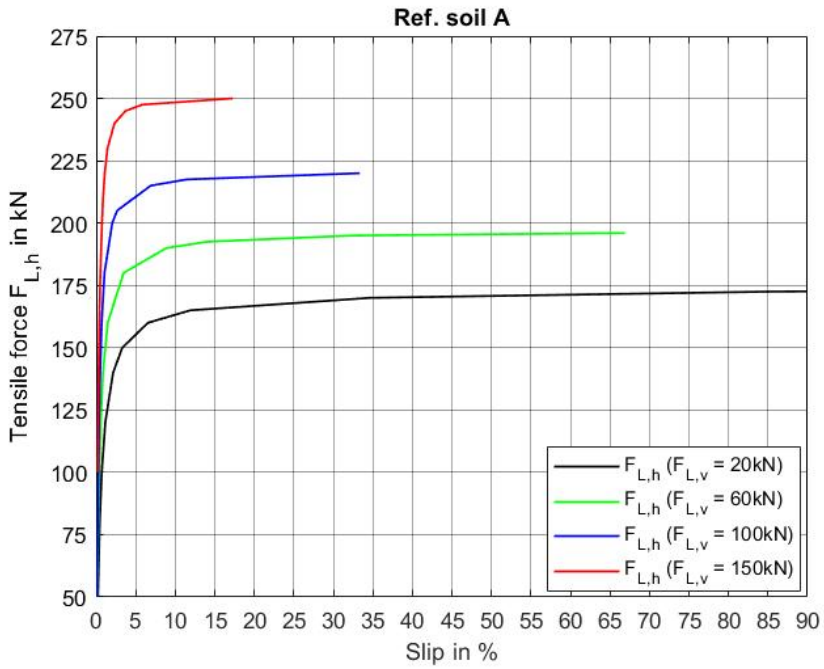

Figure 7: Reference soil A: tensile force – slip behavior

Conclusion

In summary, it was shown in this work that the relationships within such trenchless-working machines with crawler tracks as well as the interactions with the soil can be described with sufficient accuracy using simulation models.

The mechanics of the chassis and the kinematics can be illustrated very well using multi-body models. However, research on the tool-soil interaction of trenchless-working tools showed that most models are not suitable for this specific application. The mathematical-physical approach for subsoilers according to Balaton enabled an approximate description of the tools. It is possible to vary all relevant tool parameters such as working depth, angle of attack and cutting angle as well as tool width for different soil parameters and to examine the effects on the overall system. Further field studies with the tools will enable optimization of this model.

In the context of the traction behavior of the crawler track, the research showed that the analytical descriptions of these relationships by different authors mostly refer to the known approach according to Bekker. This fundamental theory, which has been developed through various works over the years, enables access to the description of these interdependencies. With the empirical parameters documented by Wong, the behavior of different crawler tracks on different soils can be analyzed very well. For this purpose, these approaches were adapted and expanded according to the given application and the non-uniform stress distribution. In contrast to existing experience, this theory neglects a separate calculation of the influence of friction on the traction-slip behavior. For the application of this model on real soils, the aim is to consider these parts as an additional degree of freedom in the

iterative determination of the empirical parameters. This should enable a better correspondence with real processes.

Regardless of the most exact possible mapping of the behavior on specific soils, this model enables the concept analysis of a traction management system for such machines. With the described relationships, it is possible to analyze the effects of changes in tool parameters on the overall system and traction behavior. As a result, control strategies for the active optimization of the traction-slip behavior by tool adjustment can be examined. In this context, useful control parameters can be identified and the limits of such a system can be shown.

References

Balaton, J. (1990): Dimensioning And Draft Force Requirement For Subsoilers. Periodica Polytechnica Mechanical Engineering 34(3-4), pp. 161–170

Bekker, M. G. (1956): Theory of Land Locomotion – The mechanics of vehicle mobility. Ann Arbor, The University of Michigan Press, Michigan

Bekker, M. G. (1960): Off-the-Road Locomotion. Ann Arbor, The University of Michigan Press, Michigan

Bekker, M. G. (1969): Introduction to Terrain-Vehicle Systems. Ann Arbor, The University of Michigan Press, Michigan

Demian, T. F. (1974): Untersuchungen an einfachen Bodenschneidwerkzeugen insbesondere für grabenlos arbeitende Dränmaschinen ausgeführt an einfachen Modellen. Dissertation, Georg-August-Universität, Göttingen

Dörfler, G. (1995): Untersuchungen der Fahrwerk – Boden – Interaktion zur Gestaltung von Raupenfahrzeugen für die Befahrung weicher Tiefseeböden. Dissertation, Universität Fridericiana, Karlsruhe

Engel, J.; Lauer, C. (2017): Einführung in die Boden und Felsmechanik – Grundlagen und Berechnungen. Carl Hanser Verlag, München

Getzlaff, G. (1951): Messung der Kraftkomponenten am Pflugkörper. Grundlagen der Landtechnik, H. 1(1951), S. 16–24

Godwin, R. J.; Spoor, G. (1977): Soil Failure with Narrow Tines. Journal of Agricultural Engineering Research 22(3), pp. 213–228

Grosa, A.; Henke, M.; Kluge, J.; Herlitzius, T. (2018): Agrothermie – Minimal Invasive Einrichtung von Geothermie-Netzen unter landwirtschaftlich genutzten Flächen. In: 76. Internationale Tagung – LAND.TECHNIK 2018, VDI-MEG, 20.–21.11.2018, Leinfelden-Echterdingen

Herlitzius, T.; Schubert, J.; Mohn, T.; Busch, D. (2015): Entwicklung flexibler Verlegetechnologien sowie Konstruktion und Bau modularer Verlegetechnik zur agrothermischen Flächenerschließung – AgroFlexWeb. Abschlussbericht, TU Dresden

Janert, H. (1955): Der Greifswalder Rohrpflug und seine Arbeitsweise. Wasserwirtschaft-Wassertechnik 5(4), S. 123–130

Janosi, Z.; Hanamoto, B. (1961): The analytical determination of drawbar pull as a function of slip for tracked vehicles in deformable soils. Proceedings of the 1st International Conference on the Mechanics of Soil – Vehicle Systems, Torino, Italy, Edizioni Minerva Tecnica

Kacigin, V. V.; Guskov, V. V. (1968): The basis of tractor performance theory. Journal of Terramechanics 5(3), pp. 43–66

Kalbheim, G. (2005): Spezialisten verlassen die Nische. Grabenfräsen, Pflüge und Drainagemaschinen. Straßen- und Tiefbau 59(5), S. 12–15

Kuhlewind, C. (1932): Die neuzeitliche Entwicklung des Maulwurfpfluges und seine Einwirkung auf den Dränbau. Dissertation, Landwirtschaftliche Hochschule Poppelsdorf, Bonn

Kunze, G.; Göhring, H.; Jacob, K. (2009): Baumaschinen / Erdbau- und Tagebaumaschinen. Vieweg + Teubner, Wiesbaden

König, K. (2017): Agrothermie – Wärme aus dem Acker. IVV immobilien vermieten & verwalten 5, S. 40–43

Lang, H.-J.; Huder, J.; Amann, P.; Puzrin, A. M. (2007): Bodenmechanik und Grundbau – Das Verhalten von Böden und Fels und die wichtigsten grundbaulichen Konzepte. Springer, Berlin, Heidelberg, New York

Merhof, W.; Hackbarth, E.-M. (Hrsg.) (2015): Fahrmechanik der Kettenfahrzeuge. Universität der Bundeswehr München, Neubiberg

Oida, A. (1979): Study on equation of shear stress – displacement curves. Report No. 5, Japan, Farm Power and Machinery Laboratory, Kyoto University

Reece, A. R. (1965): Principles of soil – vehicle mechanics. Proceedings of the Institution of Mechanical Engineers, Vol.180, Part 2A 2, pp. 45–67

Terzaghi, K. (1943): Theoretical Soil Mechanics. John Wiley & Sons, Inc., New York

Voss, B.; Zimmermann, F. (1974): Zugkraftbedarf und Verlegegeschwindigkeit grabenlos arbeitender Dränmaschinen. Wasser und Boden 26(4), S. 98–102

Wong, J. Y. (2010): Terramechanics and off-road vehicle engineering : terrain behaviour, off-road vehicle performance and design. Butterworth-Heinemann, Oxford

Wong, J. Y. (1983): Evaluation of soil strength measurements. NRCC Report No. 22881, National Research Council of Canada

Wong, J. Y. (1980): Data processing methodology in the characterization of the mechanical properties of terrain. Journal of Terramechanics 17(1), pp. 13–41

Wong, J. Y.; Harris, P. S.; Preston-Thomas, J. (1981): Development of a portable automatic data processing system for terrain evaluation. Proceedings of the 7th International Conference of the International Society for Terrain – Vehicle Systems III, pp. 1067–1091

Wong, J. Y., Preston-Thomas, J. (1983): On the characterization of the shear stress – displacement relationship of terrain. Journal of Terramechanics 19(4) pp. 107–127

Authors

Dipl.-Ing. (FH) David Wildner is a research fellow at the Centre for Applied Research and Technology, Friedrich-List-Platz 1, 01069 Dresden, E-Mail: david.wildner@htw-dresden.de

Prof. Dr.-Ing. habil. Thomas Herlitzius is Director of the Institute of Natural Materials Technology and holds a professorship at the Technical University Dresden, Bergstraße 120, 01069 Dresden

Prof. Dr.-Ing. Torsten Berg is a project manager at the Centre for Applied Research and Technology and holds a professorship at the University of Applied Sciences Dresden, Friedrich-List-Platz 1, 01069 Dresden

Notes

This project is co-financed by tax funds based on the budget decided by the members of the Saxon State Parliament and the European Social Fund.